Arch. Metall. Mater. **70** (2025), 2, 1011-1018

DOI: https://doi.org/10.24425/amm.2025.153506

V.N.S.U. VISWANATH AMMU[1,2], P.M. PADOLE[1], A. AGNIHOTRI[2], RAVIKUMAR DUMPALA[1*]

EFFECT OF RAM SPEED ON THE INTEGRITY OF AA6063 EXTRUDED PROFILE THROUGH PORTHOLE DIE

In aluminium extrusion, porthole dies are extensively used for hollow profiles production. In this work, a porthole die with three portholes around the die centre was used to produce Aluminium Magnesium Silicon based AA6063 alloy profile. Press trials were conducted using horizontal type extrusion press of capacity 690 Ton under different ram speeds i.e. 2, 4.5 and 6 mm/s for producing profiles. Subsequently, the profiles produced were aged at 175°C for 6 hours and microstructures were observed. Further, samples drawn from extruded profiles were tested for tensile properties and hardness. X-ray diffraction (XRD) analysis was carried out for identification of phases. Further, the profiles produced were evaluated for weld strength integrity using wedge expansion test. Results indicated that grain refinement has occurred while extruding the samples from billet with initial grain size of 67 μm to profiles. Also, compression load in wedge expansion test was recorded for profiles produced at a ram speed of 2 mm/s with 22.74 ± 0.92 kN with decreasing trend of compression load for profiles extruded at 4.5 mm/s and 6 mm/s, which indicated that lower ram speed produces profiles with high weld strength integrity.

Keywords: Extrusion; ram speed; porthole die; wedge expansion; tensile characteristics

1. Introduction

Aluminium and its alloys are extensively used in architectural, construction, transportation, aerospace etc., applications that requires specific strength comparable to steel, good corrosion resistance, electrical conductivity, excellent surface finish etc. [1,2]. Aluminium extrusion process offers high flexibility to produce complex geometries, products with good mechanical properties and produces lengthier profiles with constant cross section compared to other manufacturing processes [3,4]. With widespread use of extruded profiles for various new applications, there is a constant demand to produce high-quality profiles. In this regard, manufacturers are required to meet consistent product quality requirements and encountered with productivity challenges also. Hence, the process parameters that determine the metal flow, extrusion load, needs to be closely controlled to meet the intended profile quality [5,6]. In this regard, research efforts were made to study the effect of alloy chemical composition, thermomechanical parameters on metal flow, profile temperature. Alloy chemistry is an important parameter where higher ram speeds and higher extrusion ratios are possible to achieve in AA6xxx series alloys compared to high strength alloys [7]. Moreover, complex profiles are easier to achieve in softer alloys than using harder alloys [8]. Influence of process parameters during extrusion were studied based on numerical simulations and it was found that ram speed has higher effect on extrusion load [9]. Also, Arbitrary Lagrangian Eulerian (ALE) based simulation method was utilised to study the effect of ram speed on the surface defects and profile quality [10]. An incremental Proportional-Integral-Derivative (PID) control algorithm was implemented for maintaining controlled ram speed to reduce temperature of profiles [11].

Aluminium extrusion through porthole dies is extensively used for producing variety of hollow profiles. Porthole die extrusion offers great advantage in extrusion of hollow profiles in comparison with conventional route with a mandrel on stem. The process enables to produce lengthier profiles. Aluminium metal under plastic state container flows through the portholes which gets divided among the number of portholes and welded by high pressure inside welding chamber [5,12]. The process involves number of metal streams under the high pressure and temperature conditions from the portholes gets welded together inside

[1] DEPARTMENT OF MECHANICAL ENGINEERING, VISVESVARAYA NATIONAL INSTITUTE OF TECHNOLOGY, NAGPUR 440010, INDIA
[2] JAWAHARLAL NEHRU ALUMINIUM RESEARCH DEVELOPMENT AND DESIGN CENTRE, MINISTRY OF MINES, GOVERNMENT OF INDIA, AMRAVATI ROAD, WADI, NAGPUR 440023, INDIA

* Corresponding author: ravikumardumpala@mec.vnit.ac.in

weld chamber of porthole die to produce a profile of desirable configuration [12-14]. Porthole die design involves many die design variables for control of metal flow, velocity uniformity and defect free profile. Many researchers have carried out work to correlate design variables of die with respect to profile uniformity and integrity [15,16]. In this regard, weld seams are produced along longitudinal direction in porthole die extrusion [5,17]. Extruded profiles must essentially meet weld strength quality criterion for their use in high end applications and profiles must withstand post-extrusion operations which would otherwise limit their usage. Accordingly, tensile properties of profile were used as indirect way of measurement to determine profile weld quality [15,18]. Also, few researchers have estimated profile weld quality by testing sub size specimens drawn along the thickness direction of weld seams [19]. However, wedge expansion and bulge tests were used to estimate the weld quality in extruded tube profiles [20]. Accordingly, the testing parameters which can significantly influence the test results were studied by comparison of both methods to test AA7003 extruded tubes. In this regard, the wedge expansion test was found to be simple and efficient method for estimation of weld strength.

Hence, effect of ram speed has significant effect on the surface finish, due to increased deformation rate, friction that may cause surface defects, increased extrusion load requirements, temperature due to high deformation heat generation and potentially effect the mechanical properties of the profile [8,16]. However, limited literature has been reported about the effect of ram speed on the mechanical properties of extruded profiles.

In this technical work, AA6063 profiles were extruded by 690 Ton horizontal press under different ram speeds i.e. 2, 4.5, 6 mm/s. Further, the profiles were aged at 175°C for 6 hours under industrial processing conditions. In this regard, the microstructure for the profiles produced at different extrusion speeds were measured by optical microscopy. Further, XRD analysis, Vickers micro hardness and tensile properties were determined for the profiles. Subsequently, the profiles were evaluated for weld strength quality in wedge expansion test.

2. Materials and methods

The billets used for extrusion were produced industrially by Vedanta Limited using advanced casting system and homogenised after casting. Initially, the billets were Ø152 mm and machined to Ø105 mm to extrude on a press of container size 104 mm, and of length 306 mm. Billets composition was determined by Optical Emission Spectrometer. From the analysis, the alloy contains 0.51% by weight of Magnesium, 0.41% Silicon, 0.15% Iron, 0.012% Manganese etc, which conforms to AA6063 specifications.

A porthole with three portholes around the die centre was used for the studies as shown in Fig. 1. Porthole has two parts i.e. male die and female die and since the profile is produced by joining of weld seams inside weld chamber, weld integrity needs to evaluated [13,21]. Accordingly, fabrication of dies and trials were taken up on a horizontal extrusion press capacity 690 Ton. AA6063 alloy consists of Magnesium and Silicon as major alloying elements and is highly extrudable with higher limits for extrusion in terms of ram speed. In this regard, various researchers have carried out their studies up to a maximum extrusion speed of 10 mm/s. Accordingly, in the present work, ram speed values were chosen well below 10 mm/s [10,22-24]. The billets heated to specified temperature prior to extrusion inside furnace for four hours. Similarly, dies were subjected to heating at 480°C before loading in press. During press trial, the hydraulic pressure generated during extrusion was used as an indicator of extrusion load and the measurement of pressure was carried out by the instrument attached to extrusion press. The ram speed variation was achieved by varying the rate of application of hydraulic press by means of controls available

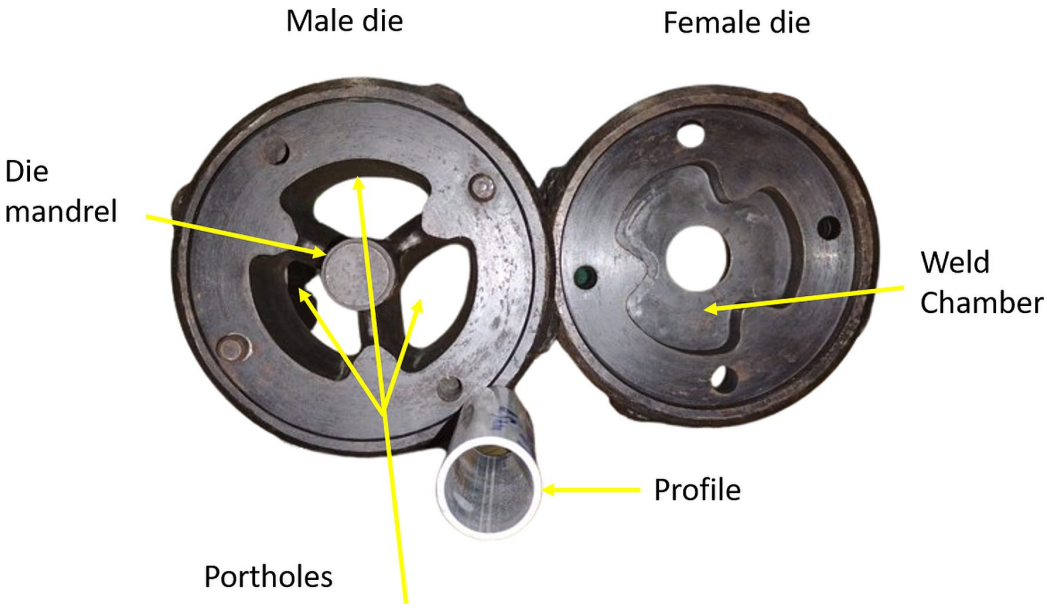

Fig. 1. Porthole die used for extruding the hollow profiles

at press control panel. Extrusion ratio represents the extent of reduction from billet to profile and given as

Extrusion ratio, R = Billet area/Profile area =

$$= (\pi / 4) d^2 \left\{ (\pi / 4) d_b^2 \right\} \Big| \left\{ (\pi / 4) \left(d_0^2 - d_i^2 \right) \right\} \quad (1)$$

where d_b billet diameter and d_i, d_o are inner and outer diameters of profile respectively.

Here, billet diameter was 105 mm, profile has nominal outer diameter 29.4 with 2 mm wall thickness. Hence, the calculated extrusion ratio from Eq. (1) was 50.28.

2.1. Microstructure, microhardness, and X-ray diffraction analysis (XRD) of the samples

The microstructure of base material i.e., billet, extruded profiles under various ram speeds after aged state were studied using optical microscope. The samples for microstructure were etched using Keller's reagent for approximately 130 seconds, and grain size was observed. Further, during Vickers microhardness test on billet, profiles samples a dwell time of 15 seconds was used by application of 100 gf load on the flat surface.

2.2. X-ray Diffraction analysis(XRD)

A comprehensive XRD analysis was carried out for AA6063 alloy in billet form, profiles produced at different ram speeds 2, 4.5 and 6 mm/s after ageing. X-ray diffraction was carried out on Rigaku equipment from Japan, utilizing Cu Kα radiation in the 2ɵ ranging from 30° to 100° and the scan rate of the data was 0.020 degree per minute while analysing the samples.

2.3. Weld strength assessment by wedge expansion test

Wedge expansion test was conducted on all extruded profiles for weld strength determination. Extruded profiles were industrially produced at different ram speeds i.e. 2, 4.5 and 6 mm/s. the profiles were forced air quenched after extrusion to room temperature and further aged at 175°C for six hours. A conical plunger was attached to the Universal testing machine (UTM) as shown in Fig. 2 for the wedge test.

Aluminium Magnesium and Silicon based alloys are usually subjected to artificial ageing treatment subsequent to extrusion in the temperature range of 150 to 200°C [25] based on the alloy chemistry and heat treatment facilities available. In the present work, aging time and temperature were referred from literature [23,26].

3. Results and discussions

3.1. Microstructure of billet and profiles extruded at different ram speeds

In porthole die extrusion, metal under the action of high compressive forces flows through the porthole portion of the die, gets divided into many metal streams depending on the number of portholes designed. Further, the streams of metal gets joined together in weld chamber portion of die under high temperature and pressure conditions [5]. The solid state bonding process is being governed by variation in parameters such as billet preheat temperature, pressure, die design, ram speed etc. [5]. Accordingly, the profiles develop different microstructural and mechanical properties due to different thermo-mechanical histories [14]. The optical micrographs showed in Fig. 3 indicated coarser microstructure with dendrites throughout the billet, while a fully recrystallized microstructure with equiaxed grains emerged after extrusion and confirms material recrystallization during extrusion.

The grain size was determined by ASTM E112 method and for the measurement of planar grain size, intercept method was used. The procedure involved metallographic sample preparation and capturing of micrograph. Further, number of parallel lines are drawn in the sample and the number of grain boundary intersections with the grains was counted to obtain mean inter-

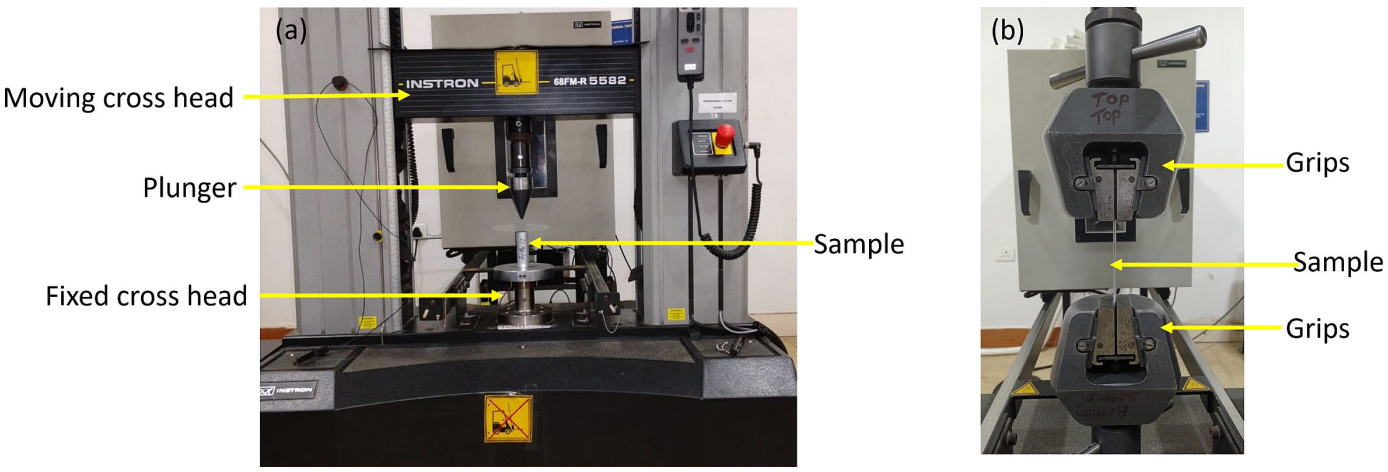

Fig. 2. (a) Wedge expansion test setup (b) tensile test setup

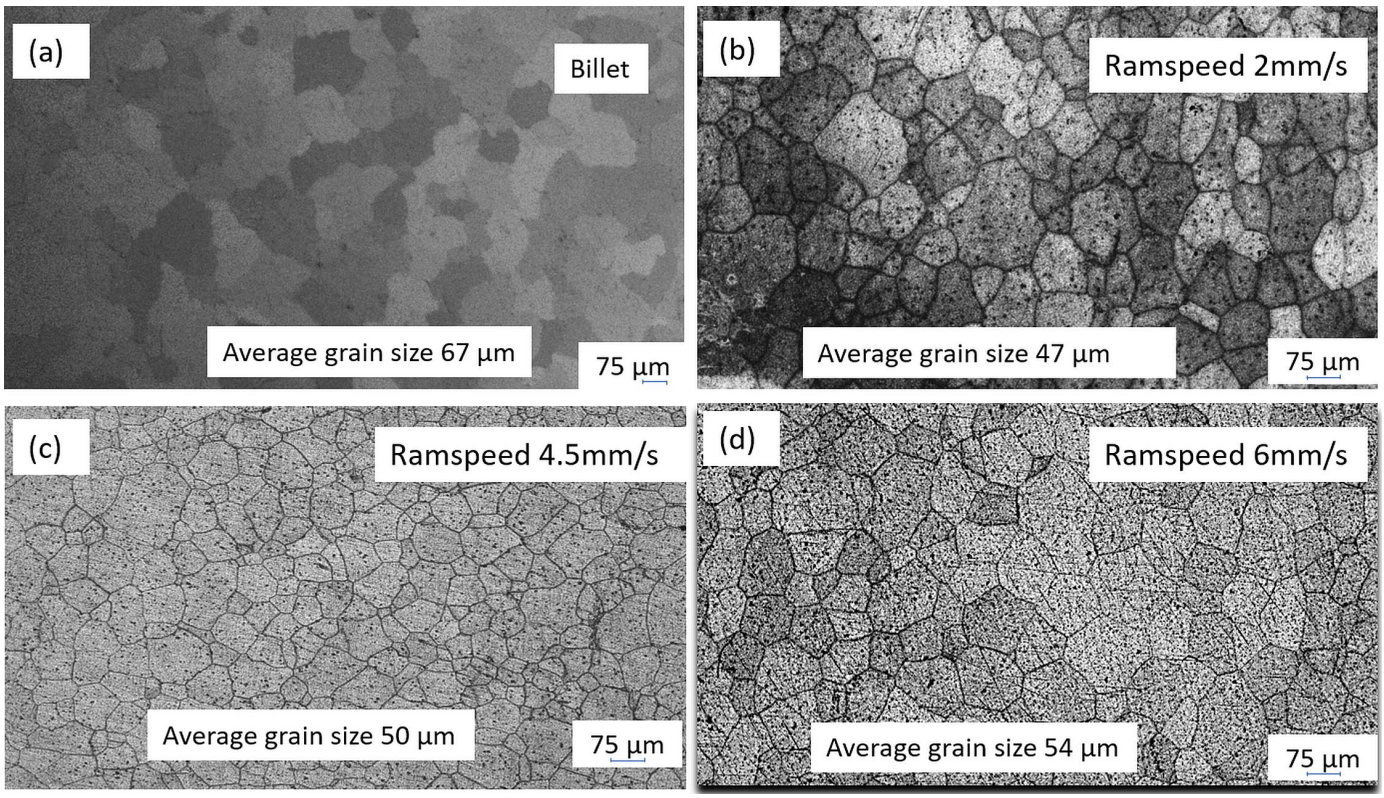

Fig. 3. Microstructure of (a) billet, profiles produced at ram speeds followed by ageing (b) 2 mm/s (c) 4.5 mm/s and (d) 6 mm/s

cept length. However, if there are more than one intersection, the number of grains to be counted were 1.5 instead of one. This measurement resulted in grain size of about 67 µm for the billet, followed by 47 µm, 50 µm and 54 µm for the profiles extruded at 2 mm/s, 4.5 mm/s and 6 mm/s respectively. From grain size, grain refinement was observed from billet to extruded samples which led to development of fine grains. The grainsizes for the profiles extruded at ram speeds 2 and 4.5 mm/s indicated grain sizes of 47 and 50 µm. However, the profiles extruded at 6 mm/s, have indicated higher grain size i.e. 54 µm, which indicates that there is a further growth of precipitates during ageing. In AA6063 alloy during ageing, there is precipitation hardening during aging treatment [27-31]. Increase in ram speed increases the extrusion load requirements as well as generates more deformation heat and heat generated is indicated in the profile temperature rise at the die exit which were evident from various studies [7,32]. Accordingly, growth of precipitates might have occurred in the samples which was indicated by variation in the grain size for the profiles extruded at different ram speeds. In this regard, ram speed increase must have resulted in grain growth due to higher heat of deformation in extrusion itself. Subsequently, ageing treatment must have further assisted in grain growth which was indicated in the increase in grain size number shown in Fig. 3(d) [33].

3.2. XRD analysis

X-ray diffraction was carried out for the billet, profiles produced at 2, 4.5 and 6 mm/s respectively as shown in Fig. 4, which indicates various peaks based on the number of precipitates formed for the alloy.

AA6063 alloy primarily contains Magnesium (Mg) and Silicon (Si) as major alloying elements with face-centered cubic (FCC) structure of aluminium. XRD peaks with this FCC phase are typically found at specific 2θ values corresponding to the planes (111), (200), (220), (311) and (222). Extrusion causes grain orientation in the material, which affects the intensity of XRD peaks [34,35]. Further, due to alignment of crystallographic planes in the extrusion direction, enhanced peak intensities were observed for specific planes.

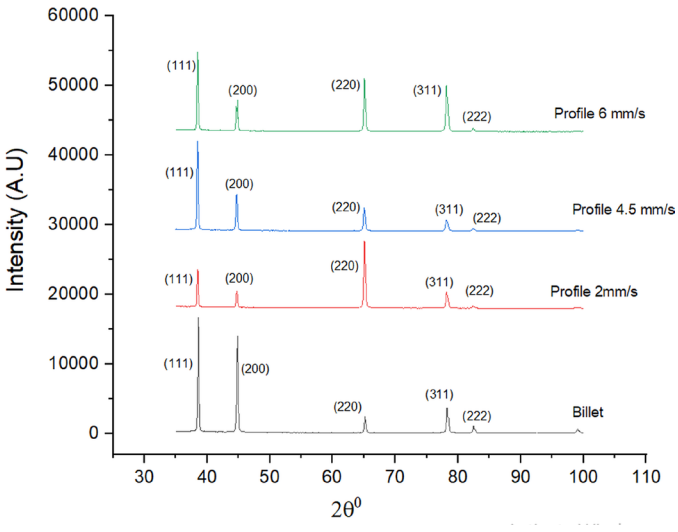

Fig. 4. XRD analysis of profiles produced at different ram speeds

3.3. Tensile properties and Vickers hardness of profiles

The tensile properties were determined according to ASTM E8 by drawing three samples in the longitudinal direction of profiles. Ultimate tensile strength (UTS) for the samples was 240.52 ± 2.02 MPa for the profiles extruded at 2 mm/s and for the samples extruded at 4.5 mm/s it was 238.28 ± 0.75 MPa and samples extruded at 6 mm/s exhibited UTS of 243.59 ± 1.89 MPa. 0.2% Yield strength (YS) was 225.42 ± 1.72 MPa for the profiles extruded at 2 mm/s followed by profiles extruded at 4.5 mm/s 217.81 ± 0.55 MPa and for the profiles extruded at 6 mm/s have YS of 226.62 ± 2.62 MPa. There is a decreasing trend in Ultimate Tensile Strength (UTS) for the profiles extruded at 4.5 mm/s ram speed compared to 2 mm/s ram speed and then UTS increased for the samples extruded at 6 mm/s and similar trend has been observed for Yield strength (YS) as shown in Fig.5. Ductility improvement has been observed for the samples with increase in ram speed and highest ductility was observed for the profiles extruded at 6 mm/s ram speed as shown in Fig. 5 and Fig. 6.

Vickers microhardness was measured at 87 HV, 84 HV and 86 HV for the profiles extruded at 2, 4.5 and 6 mm/s respectively. Thus, the finer grained structure contributes significantly to improved mechanical properties such as strength and hardness.

3.4. Wedge expansion test

The profile has outer diameter 29.4 mm and inner diameter 25.4 mm. To prevent buckling of samples during wedge expansion test, the length to diameter ratio was maintained below 3

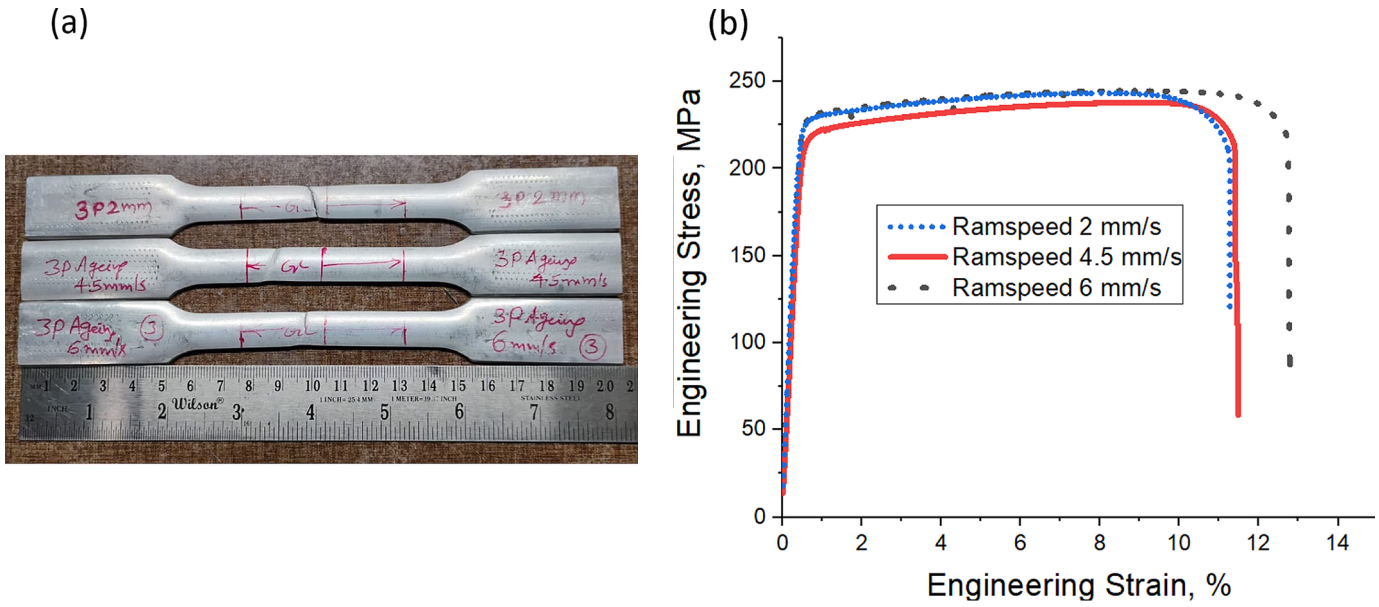

Fig. 5. (a) Tensile samples after fracture (b) Engineering stress-strain graphs for samples extruded at 2, 4.5 and 6 mm/s ram speed

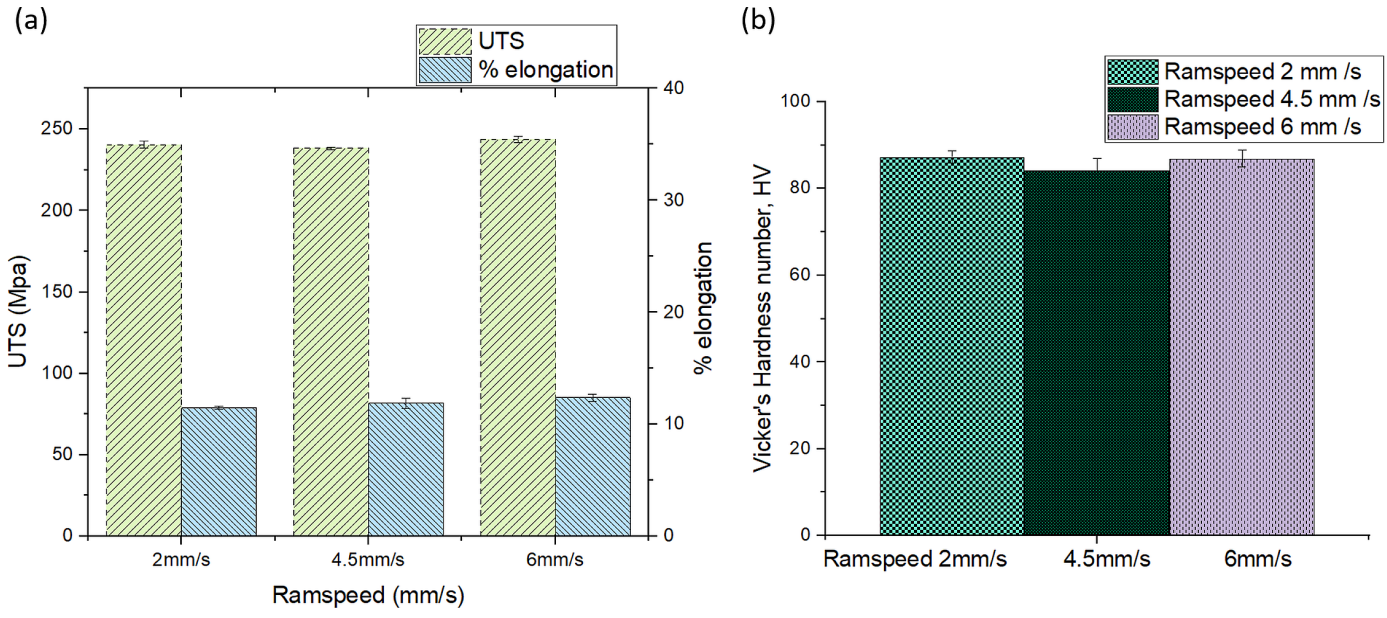

Fig. 6. (a) Tensile properties (b) Vickers micro hardness test for the profiles produced at different ram speeds i.e. 2, 4.5 and 6 mm/s

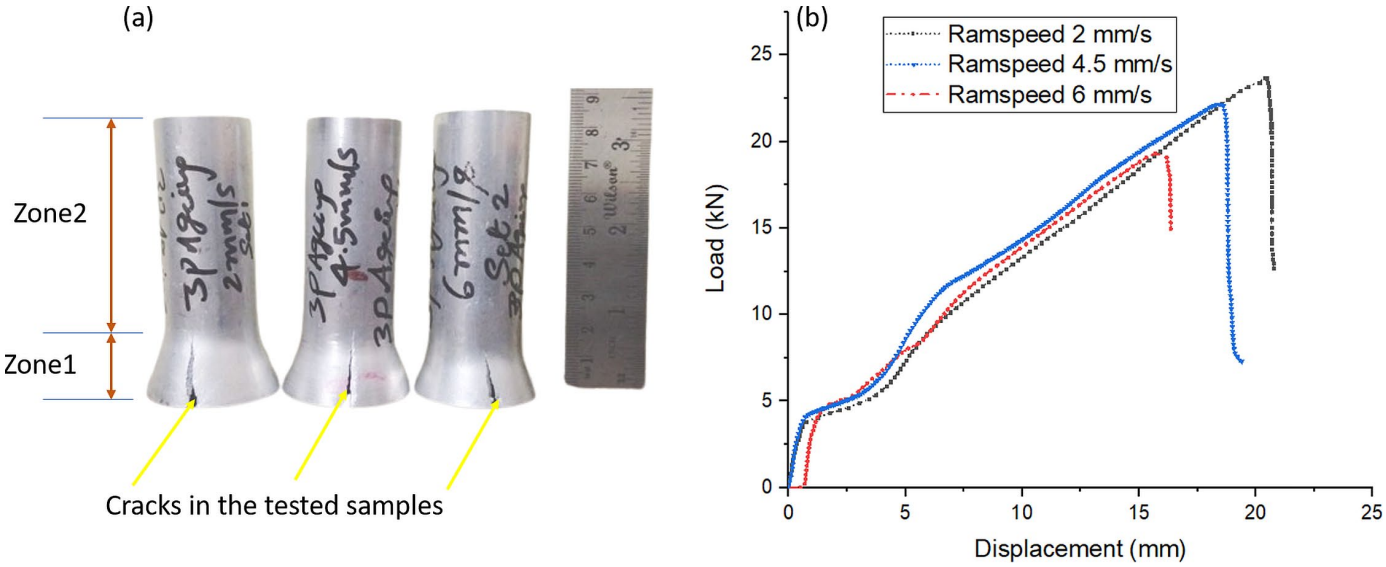

Fig. 7. Wedge expansion test, (a) tested samples and (b) load vs. displacement plot

and accordingly profile length was about 86 mm. To ensure application of low strain rate during test, the plunger attached to moving crosshead was constantly moved at a rate of at 0.5 mm/s until load drops below 40% prior to failure of profile. During the test, MOS_2 for lubrication was applied at inner portion of the profile where the plunger makes contact. Three replicas of samples were tested for each ram speed of profiles produced for weld seam quality evaluation of profiles. The load versus displacement graph for all the samples was shown in Fig. 7.

The graph indicates a first peak after the conical shaped plunger just touches inner surface of profile. With further advancement in the plunger in the downward direction, a gradual increase in load was observed until occurrence of fracture in the profile. Fig. 7 indicates two different zones i.e. cracked portion and undeformed portion in the tested profiles extruded at specified ram speeds. When the profile was subjected to compressive load, zone1 indicates a deformation zone where conical plunger contacts the profile inner surface and deformation occurs in this region until the onset of fracture. Hence, deformation reaches higher limit in this region and crack occurs in this region besides increase in diameter of profile. However, zone2 can be defined as no deformation zone where no deformation occurs. Accordingly, measurements carried out on the dimensions of the tested profiles for profiles indicated different cone diameters at the plunger end i.e. zone1 prior to fracture as indicated in TABLE 1.

TABLE 1

Tested profile dimensions in wedge expansion test

Ram speed, (mm/s)	Profile diameter at plunger end, (mm)
2	41.38 ± 0.26
4.5	39.96 ± 0.27
6	37.73 ± 0.13

From the TABLE 1, it can be observed that the diameter gradually decreases with respect to ram speed which indicates, higher the ram speed, the depth of penetration was less prior to fracture. Also, the length of crack was longest in the profile extruded at 2 mm/s ram speed followed by 4.5 mm/s and least in case of profile extruded at 6 mm/s as shown in Fig. 7. Maximum compression load for profiles produced at 2 mm/s was 22.74 kN and for profiles produced at ram speed of 4.5 mm/s was 21.06 kN which is about 7.4% decrease compared to profiles extruded at 2 mm/s. Also, the compression load in wedge expansion test for profiles extruded at 6 mm/s was 18.49 kN, which decreased to about 18.68% load in comparison with the profiles extruded at 2 mm/s. The results of compression load for all profiles were provided in TABLE 2.

TABLE 2

Compression load just prior to fracture

Profile produced from ram speed (mm/s)	Compression load (kN)
2	22.74 ± 0.92
4.5	21.06 ± 0.82
6	18.49 ± 0.58

Also, the plunger displacement was highest for the profiles produced at 2 mm/s compared to the other samples. This indicates that the profiles produced at 2 mm/s sustains higher loads in compression.

4. Conclusions

In the present study, a hollow profile was extruded on a 690 Ton extrusion press under different ram speeds i.e. 2 mm/s, 4.5 mm/s, and 6 mm/s using AA6063 alloy. Further, the profiles were aged at 175°C for 6 hours and characterized for grain size under optical microscopy. The profiles were characterised for X-ray diffraction analysis, and samples drawn from the profiles

were tested to determine tensile characteristics and Vickers hardness. Also, AA6063 alloy extrudates for evaluation of profile integrity by means of wedge expansion test. In this regard, the key conclusions drawn from the study were given as following:

- Optical microscopy was used for measurement of grain size under process conditions and micrographs indicated grain refinement from billet to profiles extruded at different ram speeds. The initial grain size of billet was 67 μm and grain size after extrusion was 47 μm for the profiles extruded at 2 mm/s. Further, grain size was 50 μm for the profiles extruded at 4.5 mm/s. Grain size was observed to be highest for samples extruded at 6 mm/s i.e. 54 μm.
- Tensile properties of the profiles indicated that UTS is highest for the samples extruded at 6 mm/s. However, there is an increase in ductility with respect to increase in ram speed and highest ductility was observed for profiles extruded at 6 mm/s.
- Vickers hardness test indicated that hardness slightly reduces in the profiles extruded at 2 mm/s ram speed compared to profiles extruded at 4.5 mm/s. Further, marginal increase in hardness was found for the profiles extruded at 6 mm/s.
- The wedge expansion test indicated profiles extruded at ram speed of 2 mm/s have sustained highest compression load i.e. 22.74 ± 0.92 kN followed by the profiles extruded at 4.5 mm/s 21.06 ± 0.82 kN. Profiles extruded at ram speed of 6 mm/s have sustained lowest compression load i.e. 18.49 ± 0.58 kN. This indicates that the profiles extruded at 6 mm/s sustained 18.68% lower load than the profiles at 2 mm/s. Overall, extrusion at lower ram speeds is prudent as the profiles sustain higher compression loads before fracture. From the results, it can be concluded that lower ram speeds are desirable for higher profile integrity.

The results suggest that variation of ram speed during extrusion has significant effect on both tensile properties and integrity of AA6063 alloy extrudates.

REFERENCES

[1] K. Zheng, D.J. Politis, L. Wang, J. Lin, A review on forming techniques for manufacturing lightweight complex – shaped aluminium panel components. International Journal of Lightweight Materials and Manufacture **1**, 55-80 (2018).
DOI: https://doi.org/10.1016/j.ijlmm.2018.03.006

[2] C.P. Kohar, A. Zhumagulov, A. Brahme, M.J. Worswick, R.K. Mishra, K. Inal, Development of high crush efficient, extrudable aluminium front rails for vehicle lightweighting. International Journal of Impact Engineering **95**, 17-34 (2016).
DOI: https://doi.org/10.1016/j.ijimpeng.2016.04.004

[3] C. Zhang, G. Zhao, Y. Guan, A. Gao, L. Wang, P. Li, Virtual tryout and optimization of the extrusion die for an aluminum profile with complex cross-sections. The International Journal of Advanced Manufacturing Technology **78**, 927-937 (2015).
DOI: https://doi.org/10.1007/s00170-014-6691-9

[4] D. Wang, C. Zhang, C. Wang, G. Zhao, L. Chen, W. Sun, Application and analysis of spread die and flat container in the extrusion of a large-size, hollow, and flat-wide aluminum alloy profile. The International Journal of Advanced Manufacturing Technology **94**, 4247-4263 (2018).
DOI: https://doi.org/10.1007/s00170-017-1127-y

[5] H.H. Jo, S.K. Lee, C.S. Jung, B.M. Kim, A non-steady state FE analysis of Al tubes hot extrusion by a porthole die. Journal of Materials Processing Technology **173**, 223-231 (2006).
DOI: https://doi.org/10.1016/j.jmatprotec.2005.03.039

[6] L. Donati, B. Reggiani, R. Pelaccia, M. Negozio, S. Di Donato, Advancements in extrusion and drawing: a review of the contributes by the ESAFORM community. International Journal of Material Forming **15**, 41 (2022).
DOI: https://doi.org/10.1007/s12289-022-01664-w

[7] Z. Peng, T. Sheppard, Study of surface cracking during extrusion of aluminium alloy AA 2014. Materials Science and Technology **20**, 1179-1191 (2004).
DOI: https://doi.org/10.1179/026708304225022016

[8] S. Ngernbamrung, Y. Suzuki, N. Takatsuji, K. Dohda, Investigation of surface cracking of hot-extruded AA7075 billet. Procedia Manufacturing **15**, 217-224 (2018).
DOI: https://doi.org/10.1016/j.promfg.2018.07.212

[9] C. Zhang, G. Zhao, H. Chen, Y. Guan, H. Li, Optimization of an aluminum profile extrusion process based on Taguchi's method with S/N analysis. The International Journal of Advanced Manufacturing Technology **60**, 589-599 (2012).
DOI: https://doi.org/10.1007/s00170-011-3622-x

[10] N. Park, Y. Song, G. Bae, S. Jung, J. Song, J. Lee, S. Choi, H. Lee, H. Sung, Evaluation of the effect of ram speed for extrusion of Al6063 based on ALE-based finite element analysis of L-shaped sample. Procedia Manufacturing **50**, 673-676 (2020).
DOI: https://doi.org/10.1016/j.promfg.2020.08.121

[11] J. Yi, Z.-Q. Liu, W.-Q. Zeng, Isothermal extrusion speed curve design for porthole die of hollow aluminium profile based on PID algorithm and finite element simulations. Transactions of Nonferrous Metals Society of China **31**, 1939-1950 (2021).
DOI: https://doi.org/10.1016/S1003-6326(21)65628-5

[12] F. Gagliardi, C. Ciancio, G. Ambrogio, Optimization of porthole die extrusion by Grey-Taguchi relational analysis. The International Journal of Advanced Manufacturing Technology **94**, 719-728 (2018).
DOI: https://doi.org/10.1007/s00170-017-0917-6

[13] H. Ji, H. Nie, W. Chen, X. Ruan, P. Pan, J. Zhang, Optimization of the extrusion die and microstructure analysis for a hollow aluminum alloy profile. The International Journal of Advanced Manufacturing Technology **93**, 3461-3471 (2017).
DOI: https://doi.org/10.1007/s00170-017-0720-4

[14] J. Yu, G. Zhao, W. Cui, L. Chen, X. Chen, Evaluating the welding quality of longitudinal welds in a hollow profile manufactured by porthole die extrusion: Experiments and simulation. Journal of Manufacturing Processes **38**, 502-515 (2019).
DOI: https://doi.org/10.1016/j.jmapro.2019.01.044

[15] D.Ç. Bölükbaşı, S. Aslanlar, M. Konar, Investigation of parameters affecting longitudinal seam quality of aluminum extruded profiles.

Journal of Radiation Research and Applied Sciences **16**, 100700 (2023). DOI: https://doi.org/10.1016/j.jrras.2023.100700

[16] G. Chen, L. Chen, G. Zhao, B. Lu, Investigation on longitudinal weld seams during porthole die extrusion process of high strength 7075 aluminum alloy. The International Journal of Advanced Manufacturing Technology **91**, 1897-1907 (2017). DOI: https://doi.org/10.1007/s00170-016-9902-8

[17] X. Lu, C. Zhang, G. Zhao, Y. Guan, L. Chen, A. Gao, State-of-the-art of extrusion welding and proposal of a method to evaluate quantitatively welding quality during three-dimensional extrusion process. Materials & Design **89**, 737-748 (2016). DOI: https://doi.org/10.1016/j.matdes.2015.10.033

[18] J. Lv, Z. Shi, J. Yu, W. Li, J. Lin, Analysis of solid-state welding in extruding wide aluminium hollow profiles using a new three-container extrusion system. Journal of Manufacturing Processes **94**, 146-158 (2023). DOI: https://doi.org/10.1016/j.jmapro.2023.03.048

[19] A.J. den Bakker, R.J. Werkhoven, W.H. Sillekens, L. Katgerman, The origin of weld seam defects related to metal flow in the hot extrusion of aluminium alloys EN AW-6060 and EN AW-6082. Journal of Materials Processing Technology **214**, 2349-2358 (2014). DOI: https://doi.org/10.1016/j.jmatprotec.2014.05.001

[20] B. Reggiani, L. Donati, Comparison of experimental methods to evaluate seam welds quality in extruded profiles. Transactions of Nonferrous Metals Society of China **30**, 619-634 (2020). DOI: https://doi.org/10.1016/S1003-6326(20)65241-4

[21] S. Li, L. Li, Z. Liu, G. Wang, in: Materials, 2021.

[22] S. Lou, Y. Wang, S. Qin, G. Xing, C. Su, Influences of extrusion speed in hollow aluminium alloy profile extrusion. Australian Journal of Mechanical Engineering **16**, 2-10 (2018). DOI: https://doi.org/10.1080/14484846.2016.1253250

[23] S. Karabay, M. Zeren, M. Yilmaz, Investigation extrusion ratio effect on mechanical behaviour of extruded alloy AA-6063. Journal of Materials Processing Technology **135**, 101-108 (2003). DOI: https://doi.org/10.1016/S0924-0136(02)01110-X

[24] X. Wang, G. Zhao, L. Sun, Y. Wang, H. Li, A strategy to promote formability, production efficiency and mechanical properties of Al–Mg–Si alloy. Journal of Materials Research and Technology **24**, 3853-3869 (2023). DOI: https://doi.org/10.1016/j.jmrt.2023.04.037

[25] S.J. Andersen, C.D. Marioara, A. Frøseth, R. Vissers, H.W. Zandbergen, Crystal structure of the orthorhombic U2-Al4Mg4Si4 precipitate in the Al–Mg–Si alloy system and its relation to the β′ and β″ phases, Materials Science and Engineering: A **390**, 127-138 (2005). DOI: https://doi.org/10.1016/j.msea.2004.09.019

[26] C.D. Marioara, S.J. Andersen, H.W. Zandbergen, R. Holmestad, The influence of alloy composition on precipitates of the Al-Mg-Si system. Metallurgical and Materials Transactions A **36**, 691-702 (2005). DOI: https://doi.org/10.1007/s11661-005-0185-1

[27] A.P. Sekhar, S. Nandy, M.A. Bakkar, K.K. Ray, D. Das, Low cycle fatigue response of differently aged AA6063 alloy: Statistical analysis and microstructural evolution. Materialia **20**, 101219 (2021). DOI: https://doi.org/10.1016/j.mtla.2021.101219

[28] T. Saito, E.A. Mørtsell, S. Wenner, C.D. Marioara, S.J. Andersen, J. Friis, K. Matsuda, R. Holmestad, Atomic Structures of Precipitates in Al–Mg–Si Alloys with Small Additions of Other Elements. Advanced Engineering Materials **20**, 1800125 (2018). DOI: https://doi.org/10.1002/adem.201800125

[29] S. Nandy, K. Kumar Ray, D. Das, Process model to predict yield strength of AA6063 alloy. Materials Science and Engineering: A **644**, 413-424 (2015). DOI: https://doi.org/10.1016/j.msea.2015.07.070

[30] M. Kolar, K.O. Pedersen, S. Gulbrandsen-Dahl, K. Marthinsen, Combined effect of deformation and artificial aging on mechanical properties of Al–Mg–Si Alloy. Transactions of Nonferrous Metals Society of China **22**, 1824-1830 (2012). DOI: https://doi.org/10.1016/S1003-6326(11)61393-9

[31] S.M.d. Hosseini, S.J. Hosseinipour, S. Nourouzi, H. Gorji, Effect of age hardening on the formability of 6063 aluminium alloy. Proceedings of the 10th International Conference on Technology of Plasticity, ICTP 2011, 941-944 (2011).

[32] N. Park, Y. Song, S.-H. Jung, J. Song, J. Lee, H. Lee, H.-M. Sung, G. Bae, Numerical and Experimental Investigation on the Surface Defect Generation during the Hot Extrusion of Al6063 Alloy. Materials (Basel) **14**, 6768 (2021). DOI: https://doi.org/10.3390/ma14226768

[33] S.-K. Li, L.-X. Li, H. He, Z.-W. Liu, L. Zhang, Influence of dynamic recrystallization on microstructure and mechanical properties of welding zone in Al–Mg–Si aluminum profile during porthole die extrusion. Transactions of Nonferrous Metals Society of China **29**, 1803-1815 (2019). DOI: https://doi.org/10.1016/S1003-6326(19)65088-0

[34] C. Zhang, C. Wang, Q. Zhang, G. Zhao, L. Chen, Influence of extrusion parameters on microstructure, texture, and second-phase particles in an Al-Mg-Si alloy. Journal of Materials Processing Technology **270**, 323-334 (2019). DOI: https://doi.org/10.1016/j.jmatprotec.2019.03.014

[35] F. Li, T. Zhang, Y. Wu, C. Chen, K. Zhou, Microstructure, mechanical properties, and crack formation of aluminum alloy 6063 produced via laser powder bed fusion. Journal of Materials Science **57**, 9631-9645 (2022). DOI: https://doi.org/10.1007/s10853-022-06993-4